A Mechanistic Perspective on Atom Transfer Radical Polymerization

Alfred. K.K. Fung, and Michelle L. Coote*

ARC Centre of Excellence for Electromaterials Science, Research School of Chemistry, Australian National University, Canberra, Australian Capital Territory 2601, Australia

Abstract

Since its invention 25 years ago, Atom Transfer Radical Polymerization (ATRP) has become one of the most dominant methods in controlled radical polymerization. This rise in importance is due in large part to increases in scope, reduced catalyst loading, and improved oxygen tolerance. These developments have been in turn underpinned by an improved understanding of the mechanism, kinetics and structure-reactivity trends. This mini review outlines these mechanistic developments with a particular emphasis on the relationship between structure and activity in both the catalyst and alkyl halide substrate, and their implications for future catalyst design.

Keywords

Atom Transfer Radical Polymerization; structure-reactivity analysis; ATRP catalyst design; Cross-coupling

Introduction

The use of polymers has had an immutable impact upon our daily lives, with millions of tons produced worldwide per annum. One of the critical processes in the production of polymers is free radical polymerization[1]. However free radical polymerization suffers from an inherent lack of control over dispersity and tacticity. Controlled radical polymerization (CRP) techniques have been developed in order to address this problem[2]. CRP relies upon the reversible storage of the active radical so as to reduce the number of termination events relative to the total number of polymer chains. This not only provides superior control over the molecular weight and dispersity, but also controls the chain end composition, thus allowing for the construction of specialized chain architectures such grafts, stars, blocks, and so forth[3]. There are a number of different types of controlled radical polymerization process, differing primarily in the nature of the dormant form and the reaction(s) converting it to the active form. Of these, arguably the most important are nitroxide mediated polymerization (NMP)[4], reversible addition fragmentation chain transfer polymerization (RAFT)[5] and Atom Transfer Radical Polymerization (ATRP)[6, 7]. For each of these techniques, there have been numerous reviews of their chemistry and applications. Here, we do not duplicate these, but rather focus specifically on structure-reactivity analyses of ATRP and their lessons for catalyst design.

ATRP was separately discovered by Sawamoto[6] and Matyjaszewski in 1995[7]. In its original form, it harnessed and improved upon the chemistry of atom transfer radical addition, which uses copper catalysts to generate carbon-centered radicals (R•) from alkyl halide (R-X) bonds.* **Scheme 1** shows the basic ATRP control equilibrium. Active radicals are generated from dormant alkyl halides via an inner sphere electron transfer reaction, mediated through a metal ligand complex. The equilibrium constant, K_{ATRP} is the ratio between the activation and deactivation of the mediator complex and is a key factor governing the concentration of transient radicals in solution, and hence the rate of polymerization and the extent of molecular weight control. K_{ATRP} depends on the nature of the ATRP catalyst and the strength of the R–X bond and corresponding stability of R•, which in turn depends on which monomer is being polymerized. While Cu-based ATRP is the most popular, ATRP can be executed using other metals such as Ti, Mo, Re, Fe, Ru, Os, Rh, Co, Ni, and Pd[8], and indeed Sawamoto's seminal work[6] itself made use of ruthenium catalysts. Nonetheless, Cu remains the most prominent and is the focus of the present review.

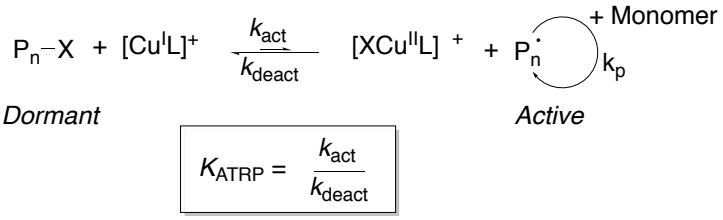

Scheme 1. Control Equilibrium in ATRP.

Mechanism

Given the fundamental stability of the carbon-halogen (R-X) bond, homolytic cleavage requires the assistance of a mediator. The use of a copper to generate a carbon centered radical (R•) is a topic

* The Cu catalyst is not strictly a catalyst but rather an activator, although it is functionally distinct from both traditional free radical initiators or the alkyl halides that are referred to initiators in the ATRP process. For clarity, we therefore retain the term catalyst throughout this review.

well explored in synthetic organic chemistry through processes such as Atom Transfer Radical Addition[9], Ullmann cross-coupling[10] and photoredox catalysis[11]. Metal mediated activation of alkyl and aryl halides to create radicals in solution could proceed in principle via four possible mechanistic pathways; oxidative insertion, inner sphere electron transfer, stepwise outer sphere electron transfer and dissociative electron transfer (Scheme 2). The relative favorability of the alternative processes is influenced by the ligands, the nature of the activation process (e.g. thermal versus photochemical versus electrochemical) and the structure of the R-X substrate. For ATRP, theory and experiment have shown that the inner-sphere mechanism is preferred.[12-14] This can be understood in terms of the very high energetic cost of electron transfer from [L_nCu^I] to the alkyl halide, which is partially compensated by the halide affinity of the Cu^{II} product. Hence a concerted ISET reaction, which avoids the high energy intermediate $[L_nCu^I]^{+\bullet}$, is typically 30 kcal mol^{-1} more favorable than the stepwise process. [14, 15] Although oxidative addition is also concerted, it is less favorable than ISET due to steric crowding around the [L_nCu^I]. This has also been shown to be true of Ullmann cross-coupling[16], although it should be noted that in some cross-coupling applications, where for example monodentate phosphines are used as ligands[17], oxidative addition is much more favorable due to the lower oxidation potential of the catalyst and reduced steric crowding.

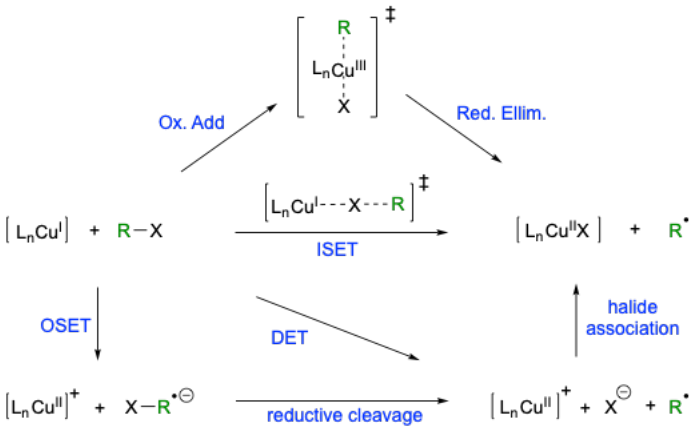

Scheme 2. Possible R–X activation mechanisms: oxidation addition (Ox. Add) followed by reductive elimination (Red. Elimin.); inner-sphere electron transfer (ISET); stepwise outer sphere electron transfer (OSET) followed by reductive cleavage and then halide association; dissociative electron transfer (DET) followed by halide association.

Mechanistic Variants of ATRP

In addition to standard ATRP, there are a number of variants that been designed to reduce catalyst loading, improve oxygen tolerance, and generally improve the industrial attractiveness of the process and broaden its scope. In reverse ATRP[18] the catalyst is added in its oxidized (Cu^{II}) state and a conventional free radical initiator is employed instead of alkyl halides (Scheme 3). Propagating radicals are generated and these react with the Cu^{II} catalyst to form alkyl halides and the reduced Cu^I catalyst, following which the process proceeds in the same manner as standard ATRP. The advantage of reverse ATRP is that the Cu^{II} catalyst is much less sensitive to air and easier to handle, thus making the process more suitable for highly active catalysts, applicable to mini-emulsions and more amenable to industry.[19, 20] The disadvantage, however, is that the non-halide end of the dormant chain bears the initiator fragment, rather than a designer functional group, which limits chain topology and functionality. To address this, simultaneous reduction and normal initiation (SR&NI) was subsequently developed (Scheme 3).[21] This is similar to reverse ATRP except that both a conventional initiator and alkyl halides are used. The decomposition of the initiator

generates a small population of the active Cu^{I} catalyst from the oxidized Cu^{II} catalyst, while the majority of the polymer chains are initiated from alkyl halide in the normal manner and can thus be easily functionalized. While SR&NI is an improvement on reverse ATRP, a small fraction of chain ends still bear initiator fragments. This problem was overcome by replacing the conventional radical initiator with a non-radical reducing agent such as ascorbic acid. In this process, known as AGET (Activators Generated by Electron Transfer), the Cu^{II} is converted to the active Cu^{I} form *in situ* by the reducing agent, while all propagating chains are initiated from the alkyl halide in the normal manner.[22] The reducing agent can also mop up any dissolved oxygen, making it suitable for a wide range of media including mini-emulsions.[23]

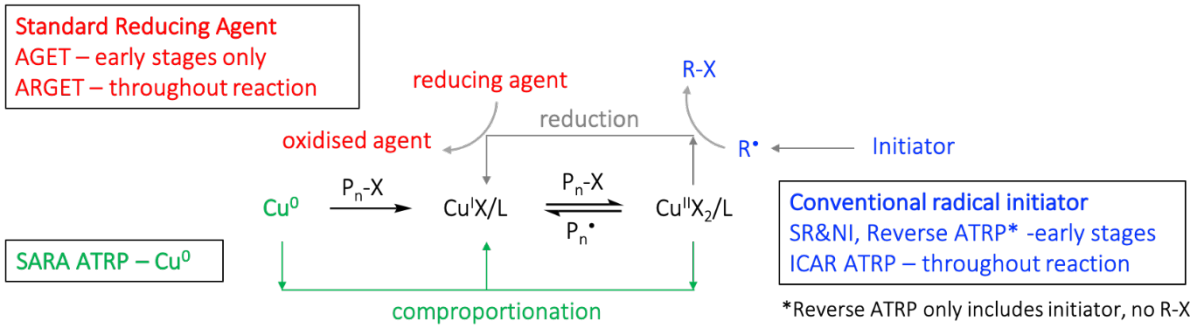

Scheme 3. Variants of ATRP

The above processes focus on altering the initial stages of the ATRP so as to generate the Cu^{I} catalyst *in situ* from the more stable Cu^{II}. However, it was soon realized that these alternative approaches to generating the Cu^{I} from Cu^{II} could also be applied throughout the entire process (Scheme 3). This supplemental re-generation provides a means of re-generating active form of the catalyst that would otherwise remain inert due to the loss of propagating radicals through bimolecular termination. This allows the process to occur with ppm catalyst concentrations, which is not only a cost saving, but also enables catalyst removal to be avoided in many applications. The use of lower catalyst concentrations also eliminates or minimizes side reactions involving the catalyst. In ARGET (Activators ReGenerated by Electron Transfer), like AGET, a non-radical forming reducing agent is used so as to ensure high chain end fidelity.[24] In ICAR (Initiators for Continuous Activator Regeneration), like SR&NI, a conventional radical initiator is used.[25] This sacrifices some of the chain end fidelity but leads to much faster reactions, with kinetics resembling conventional radical polymerization.[26] The mechanistic cross-over from AGET to ARGET, and from SR&NI to ICAR, is governed by the concentrations of supplemental activators, their reaction rates and in some cases whether or not they are slowly added throughout the process.[27]

Zero-valent metals such as metallic Cu, Fe, Mg and Zn have been shown to rapidly increase the rate of ATRP.[28-30] Two different mechanistic interpretations of their role have been put forward. Matyjaszewski et al.[28, 29, 31-33] have argued that the metal acts as both a supplemental reducing agent by reacting with the Cu^{II} in a comproportionation reaction to form the active Cu^{I} catalyst (Scheme 3). However, unlike the reducing agents used in ARGET, the metals can also directly activate alkyl halide initiators, albeit at a slower rate than Cu^{I}. Thus, the process is known as SARA (Supplemental activator Reducing Agent). In the alternative mechanistic interpretation, known as SET-LRP (Single Electron Transfer Living Radical Polymerization), Percec et al.[30] argue that disproportionation rather than comproportionation is dominant, and so there is little or no Cu^{I} present, and it is the Cu^{0} that acts as the main activator via an outer-sphere electron transfer

process, with the Cu^{II} the main deactivator.[30] There has been considerable debate as to the relative validity of the alternative mechanisms[34, 35]; however, kinetic measurements of the disproportion rate of Cu^{I} support the SARA mechanism, even in polar solvents.[33]

Other methods of supplemental regeneration, using electrochemistry,[36] photochemistry[37] and sonochemistry,[38] have also been explored. These offer various advantages over traditional methods, particularly with respect to temporal (and in the case of light also spatial) control. Their enhanced ability to control the regeneration of the Cu^{I} from Cu^{II} with an external stimulus allows the polymerizations to be essentially oxygen tolerant. For reviews of these see Refs. 36, 39, 40.

Effect of the Ligand

A common feature of ATRP copper-based mediators is their nitrogen ligands.[8] Copper(I) complexes generally form tetrahedral or square planar complexes, and hence a cationic species coordinates a tetradentate or two bidentate ligands, while neutral complexes coordinate tridentate ligands. Copper(II) species form trigonal bipyramidal structures with tetradentate and bidentate ligands; with tridentate ligands, a square pyramidal structure is formed in which the incoming group occupys the axial position[41]. The original ATRP mediator system tested by Matyjaszewski et al.[7] was CuX/bpy (2,2'-bipyridine; see Scheme 4 for the ligand structures). This was able to control the dispersity of styrene effectively, but not monomers with less stable propagating radicals such as vinyl acetate. Moreover, the reaction is relatively slow, and requires elevated temperatures[42, 43]. Structurally related ligands such as phenanthroline derivatives were also investigated, both for thermal[44, 45] and photo-activation.[46, 47] Subsequent investigations of linear and branched amines lead to the discovery of a range of cheap and highly efficient catalysts such as N,N,N′,N′′,N′′-pentamethyldiethylenetriamine (PMDETA)[48], tris(2-pyridylmethyl)amine (TPMA)[49] and tris[2-(dimethylamino)ethyl]amine (Me_6TREN)[50]. While not substantially expanding monomer scope, these ligands allowed the temperature to be decreased from 100°C to room temperature. [50] TPMA and Me_6TREN are regarded as the best catalysts of that era as they balance high reactivity, ease of synthesis and relatively fast reaction rates under mild conditions. More recently a series of new ligands based upon the TPMA backbone, such as $TPMA^{NMe2}$, have been developed with activities unparalleled by any from the previous generation of ATRP catalyst.[51, 52] Computational studies suggest that this activity could be further improved by capping of the amine ligand (e.g. using quin, ((2*R*,6*R*,7*R*)-quinuclidine-2,6,7-triyl)trimethanamine) so as to destabilize the Cu^{I} and lower its oxidation potential.[15]

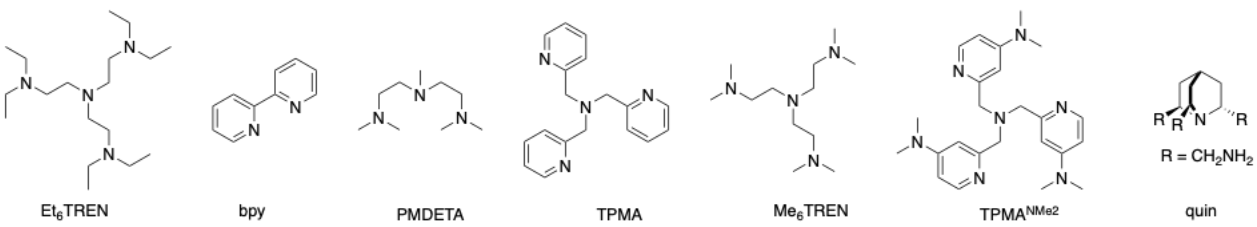

Scheme 4. Ligands used in ATRP Catalysts

To date, tetradentate amine ligands have been undeniability the best option for Cu-based ATRP mediators.[53] Phosphorus ligands have been explored experimentally[8, 54-57] and theoretically[15] without success, due to speciation issues. However, it should be noted phosphines improve the favorability of electron transfer compared with amines, albeit at the cost of both halophilicity and

ligand affinity of the Cu^{II} catalyst.[15] Phosphines can however be used with metals with high inherent halophilicity such as osmium and ruthenium in order to facilitate efficient catalysis.[54] Interestingly, recent work has shown that phosphorus ligands are suitable for Cu-based photoredox catalysts with ISET capability in small molecule reactions like cross coupling.[11]

Figure 1 shows experimental k_{act} values for $CH_3CH_2(COOCH_3)Br$ with $Cu^{I}Br$ in MeCN at 22 °C and a wide range of ligands.[51, 52, 58] These values range over 10 orders of magnitude for available ligands,[51, 52, 58] with another 3 orders of magnitude improvement in activity possible if the computationally designed ligands are considered as well.[15] A number of experimental and computational structure-reactivity studies have been published and the structure-reactivity trends are reasonably well understood. The catalytic activity depends in large part on the ability of the ligand to stabilize Cu^{II} versus Cu^{I}, and indeed excellent semilogarithmic correlations between the reduction potential of the Cu^{II} complex and K_{ATRP} have been observed.[58-60] To a first approximation, the stability of the Cu^{II} versus Cu^{I} oxidation state depends on the electron donation capacity of the ligand, with the activity of ligands decreasing in the following order: alkyl amine ≈ pyridine > alkyl imine > aryl imine > aryl amine.[58-60] Some of the most active ligands, such as $TPMA^{NMe2}$, are then further substituted with electron donating amine or methoxy substituents.[51, 52]

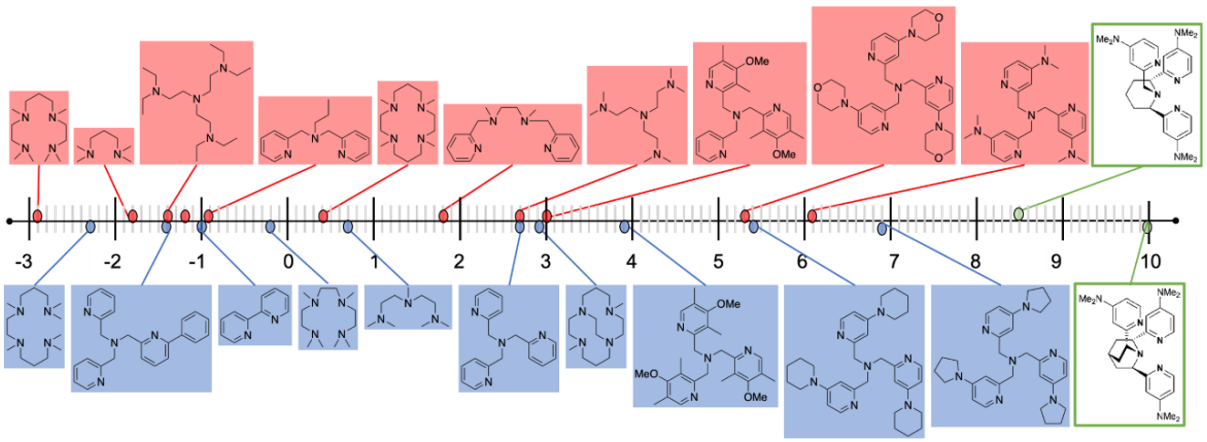

Figure 1. Selected experimental activation rate constants k_{act} (M^{-1} s^{-1}) for ATRP various N-based ligands with the initiator $CH_3CH_2(COOCH_3)Br$ in the presence of $Cu^{I}Br$ in MeCN at 22 °C. Experimental data taken from Refs [51, 52, 58]. The species in green boxes are computationally predicted values for new ligands taken from Ref. [15], other more active ligands are also predicted in this paper but these are the ones with synthetic precedent.

However, within these broad trends, there is still considerable variation with chemical structure that is best understood by examining the molecular orbitals of the Cu(I) complex (Figure 2). By Koopman's theorem, the favorability of electron transfer in ATRP depends on the energy of the highest occupied molecular orbital (HOMO) in the $[LCu^{I}]^{+}$ catalyst: the higher the energy, the more easily an electron is removed. Figure 2(a) shows, as a typical example, the highest 5 occupied orbitals in $[Cu^{I}(Me_6TREN)]^{+}$.[15] In the HOMO, there is a node between the axial nitrogen and the Cu, and hence any reduction of the distance between N and Cu leads to increased repulsion between them, resulting in turn in a destabilized HOMO and a more easily oxidized Cu^{I} catalyst.[15] Conversely, an elongation of the axial bond stabilizes the HOMO and hence raises the oxidation potential of the complex. As a result, steric factors can play a significant role in activating or deactivating the complex toward electron transfer. An extreme example is provided in Figure 2(b) which compares

the geometries of $[Cu^{I}(Me_6TREN)]^+$ with $[Cu^{I}(quin)]^+$, the latter a computationally designed complex with a predicted increase in k_{act} of 2.5 orders of magnitude relative to $[Cu^{I}(Me_6TREN)]^+$ despite the same basic substitution pattern.[15] The cage structure that caps the quin ligand sterically pushes the axial nitrogen toward the Cu resulting in a decrease the axial bond strength and a concurrent destabilization of the HOMO and decrease in oxidation potential.

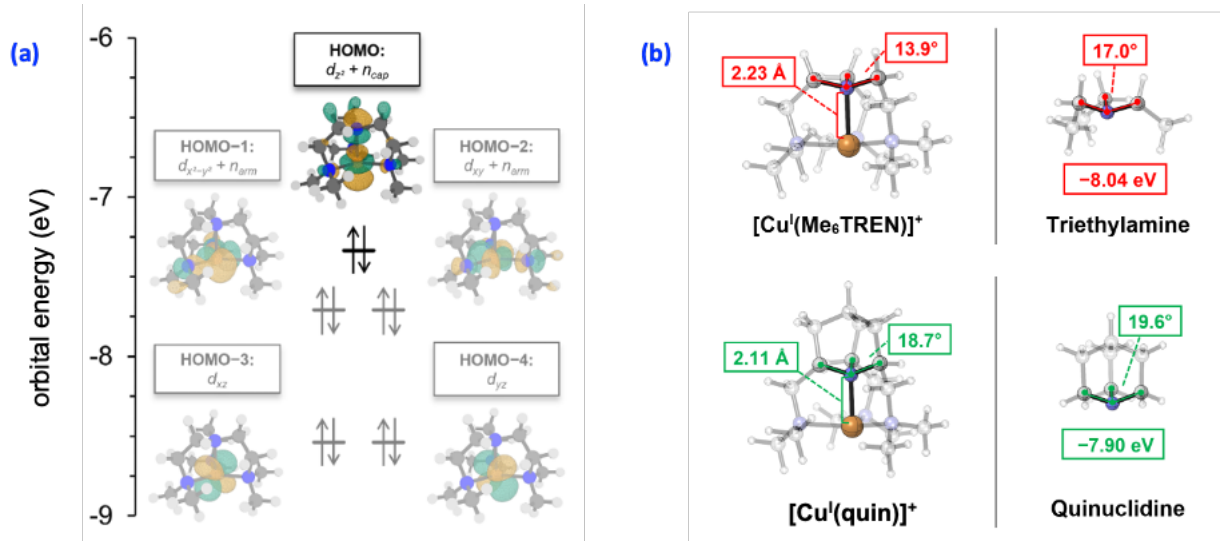

Figure 2. (a) The highest occupied orbitals in $[Cu^{I}(Me_6TREN)]^+$. (b) Geometries and POAV N-pyramidalization angles for the $[Cu^{I}(Me6TREN)]^+$ and $[Cu^{I}(quin)]^+$ complexes as well as the corresponding core structures (triethylamine and quinuclidine). Reproduced from Ref [15] with permission. Copyright (2019) American Chemical Society.

While the ability of the ligand to stabilize Cu^{II} versus Cu^{I} is the main factor governing activity, other factors also play a role. In particular, the backbone flexibility of the ligand is critical to its ability to accommodate the geometry change from the tetrahedral or square planar Cu^{I} structure to trigonal bipyramidal Cu^{II} structure.[11] Moreover, the degree of steric hindrance the ligand presents to the incoming X-R species during the reaction also dramatically affects activity, as seen in the comparison of Et_6TREN and Me_6TREN.[61] The increased steric bulk in the latter results in a decrease of the k_{act} by roughly 4 orders of magnitude because the bulkier side chains bury the reaction center. In addition to steric effects, the halophilicity of the Cu^{II} catalyst is also critical and while the largest factor governing this is the nature of halogen (vide infra), the ligands on the catalyst also play a role. For a given halogen, the halophilicity of the catalyst depends primarily on how electronegative the Cu^{II} catalyst is, with studies showing a good correlation between natural charge on the Cu^{II} and halophilicity.[15] At some level, therefore, efforts to lower the oxidation potential of Cu^{I} through electron donation are countered by detrimental effects on the halophilicity of the resulting Cu^{II}. Nonetheless, within the nitrogen-based ligands at least, the former effect dominates and stabilizing Cu^{II} versus Cu^{I} results in improvement in catalyst activity.

Effect of the Alkyl-Halide

The activity of alkyl halides (i.e., initiators and dormant propagating species) in ATRP depends on both the strength of the alkyl halide bond and the halogenophilicity of the ATRP catalyst. The bond strengths have been widely studied for unimeric radical species. A particularly large compilation of R-Cl strengths, studied quantum chemically at a consistently high level of theory, can be found in Refs 62, 63 and are collected together in Table S1 of the Supporting Information. Figure 3 (a) shows

the relationship between these bond strengths and their corresponding R-H bond strengths, calculated at the same level of theory in the same study. While is there is some correlation between the two, it is quite poor (R^2 = 0.65). Whereas the R-H bond strength is dominated by the stability of the R• radical product, the R-Cl bond has a contribution from the ability of R to stabilize the polar covalent bond through R-Cl ↔ R^+ Cl^- resonance. As a result, whereas both electron donors and acceptors stabilize R• and hence weaken R–H BDFEs, only acceptors weaken R–Cl. This is seen clearly in Figure 4(a) where some of the strongest R–Cl bonds also have some of the weakest R-H bonds. These bonds feature radical stabilizing lone donor groups such as NH_2 and OH that stabilize R–Cl, despite the high stability of R•. The reason this is of relevance to ATRP is that the inclusion of additional electron donating CH_3 groups around the radical center can sometimes counterintuitively reduce the activity of the alkyl halide, despite the fact that the extra methyl groups stabilize R• and are sterically detrimental to the bond strength. This is illustrated Figure 4 (b) which shows the bond strengths for series of primary, secondary and tertiary R-groups. In all cases, R-H bond strength decreases with increasing methyl substitution, whereas in most cases R-Cl bond strength actually increases. The rare exceptions to this are when the primary substituent is an effective electron acceptor. In those cases, captodative stabilization of R• with increasing methylation helps to counter effects on R–Cl bond strengths. In practical terms, this means that 2-phenylpropyl halides are less effective initiators for styrene polymerization than 1-phenylethyl halides, while those based on electron withdrawing acrylates, acrylamides and nitriles show reactivity trends that are less sensitive to methyl substitution than might be expected based on the corresponding R• stability trends.

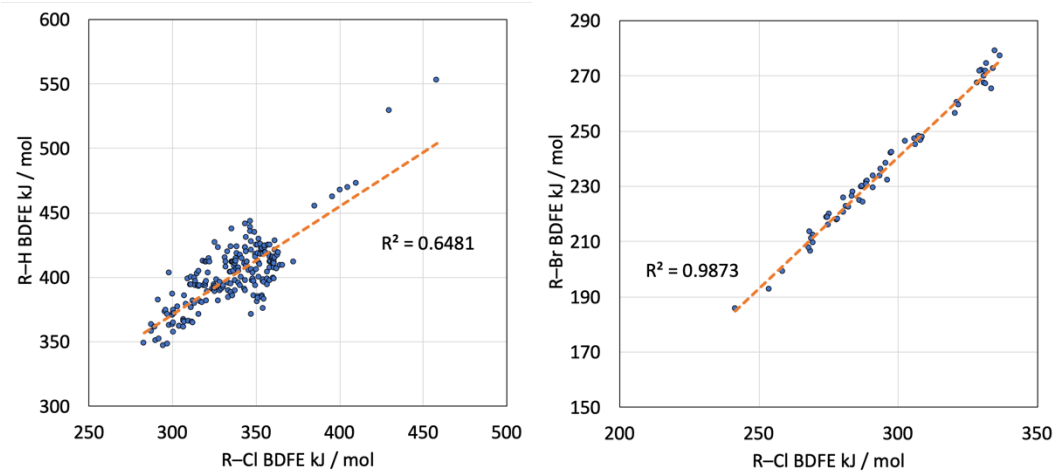

Figure 3. (a) Correlation between gas-phase R-H and R-Cl bond dissociation Gibbs free energies from Refs [62, 63]. (a) Correlation between acetonitrile R-Br and R-Cl bond dissociation Gibbs free energies from[64]All data for [64] both (a) and (b) collected in Table S1 and S2 of the Supporting Information.

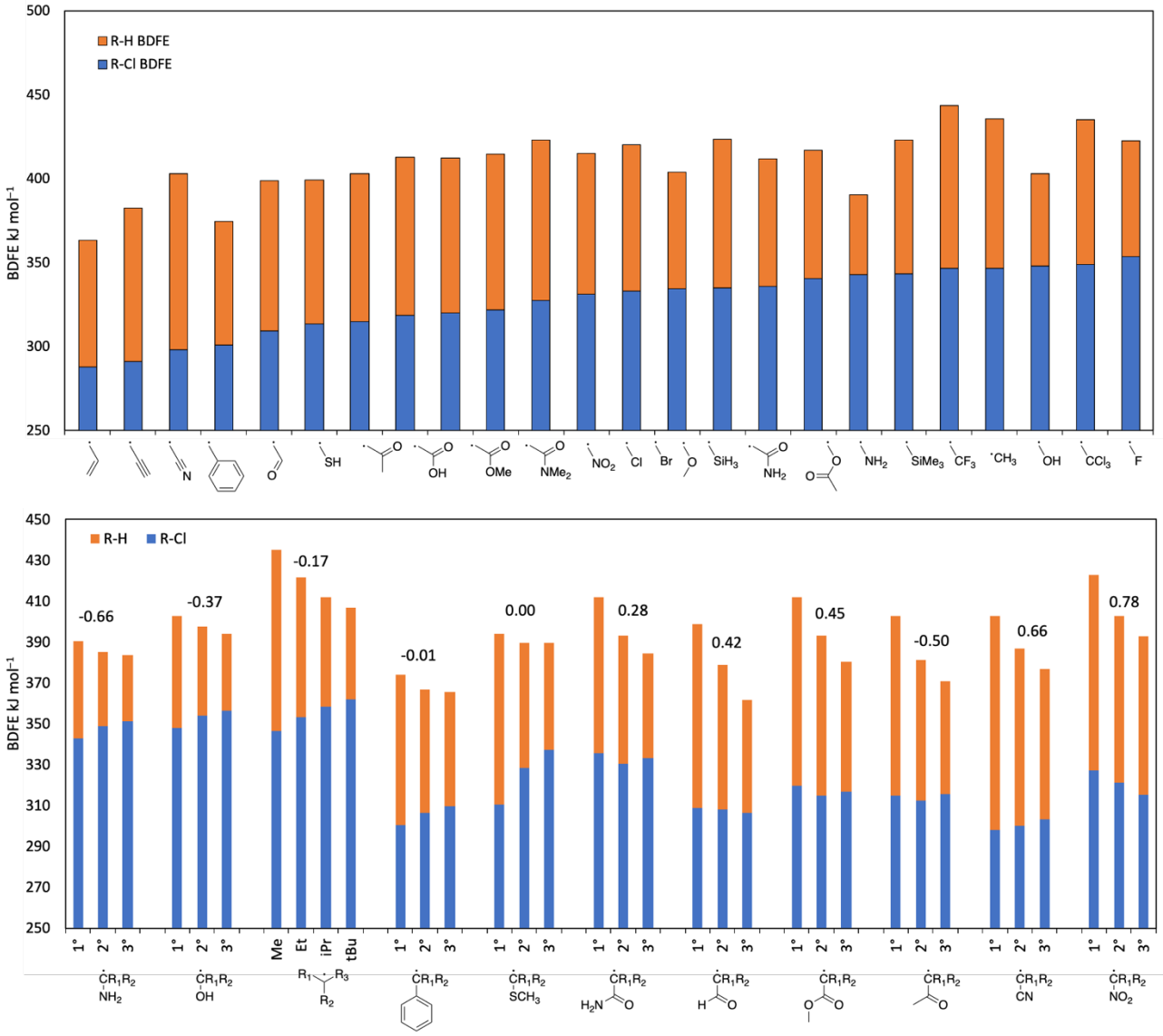

Figure 4. Selected gas-phase R-H and R-Cl bond dissociation Gibbs free energies (BDFEs, 298 K kJ mol^{-1}) from Refs 62, 63. The total column height is the R–H BDFE and the blue portion is the R–Cl BDFE, which is lower in all cases. (a) Shows a series of primary R-groups, CH_2X as a function of X; (b) shows the effect of increasing methyl substitution on CR_1R_2X (1° $R_1 = R_2$=H; 2° R_1 = H and $R_2 = CH_3$; 3° R_1=R_2=CH_3). The numbers at the top of the columns in (b) are the Hammett parameters taken from Ref 65. All data for both (a) and (b) are collected in Table S1 the Supporting Information.

Comparing next alkyl halides and bromides, Figure 3 (b) shows that their bonds well correlated with one another over a broad representative test set of substituents (R^2 = 0.99).[64] This is because both sets of bonds are polar and so are affected by donating and withdrawing groups in a similar manner. Hence the same structure-reactivity analysis outlined above for alkyl chlorides is equally applicable to the alkyl bromides. While the trends are the same, the bond strengths themselves are considerably different in magnitude with a typical alkyl bromide bond being 60 kJ mol^{-1} weaker than the corresponding halide due to poor orbital overlap.[64] This normally leads to the expectation that bromides are considerably more reactive than chlorides in radical processes. However, in ATRP activity also depends on the halogenophilicity of the ATRP catalyst, and chlorides have greater affinity for the Cu^{I} species due to their greater electronegativity.[58] As a result, differences between K_{ATRP} for corresponding halides and bromides are less than an order of magnitude. This is illustrated in Figure 5 for a set of representative experimental data, taken from Ref. 58.

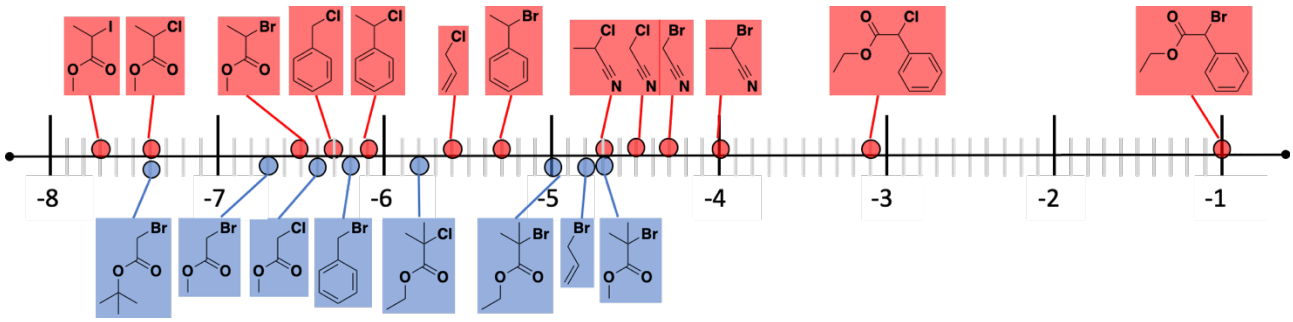

Figure 5. Selected experimental ATRP equilibrium constants for various initiators with $Cu^{I}X$/TPMA (X = Br, Cl) in acetonitrile at 22 °C. Data taken from Ref. 58. The ATRP equilibrium constant depends on the halogenophilicity of the catalyst as well as the strength of the breaking bond, which is why the R-Br species perform a lot better than expected based on their relative bond strengths.

Side Reactions

The coordination of organic radicals to the metal center is well-known and is the basis for the formation of organometallics such as the Grignard reagent.[66] In polymer chemistry, the ability to coordinate radicals to a metal center in order to generate a dormant organometallic intermediate is the basis of Organometallic Mediated Radical Polymerization (OMRP). In principle, the ATRP process occurs is in equilibrium with OMRP. Trapping of R$^{\bullet}$ serves to reduce the reaction rate but not the degree of control. Thus, in practice, OMPR is a slower process when compared to ATRP, especially when using the new generation of ATRP catalysts.[67] However, the trapping of radicals as organometallic compounds could be an important feature which reduces the risk of a runaway radical polymerization in eATRP[68] and mechanoATRP[69] where the high concentration of $LCu(I)^{+}$ and R$^{\bullet}$ can build up at the surface/solution interface.

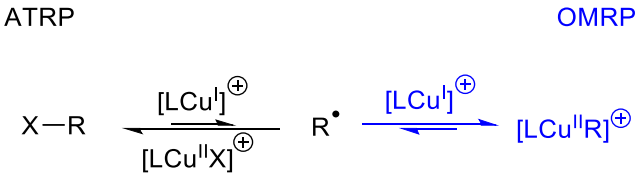

Scheme 5. ATRP versus OMRP

The effects of solvents upon the favorability of redox processes have been well studied.[70, 71] In general, polar solvents stabilize highly charged species better than non-polar solvents. Hence, the relative stability of Cu^{II} versus Cu^{I} increases with solvent polarity, and this is accompanied by an increase in k_{act}, a decrease in k_{deact} and hence an overall increase in K_{ATRP}.[72-74] Nonetheless, it should be noted the overall increases in k_{ATRP} is small in comparison to the choice of monomer/initiator.[74] Fortunately, coordinating solvents fail to compete effectively against the binding strength of conventional ATRP ligands. The halide concentration also affects ATRP. Whilst the ATRP reaction mixture contains many species, the dominant Cu(I) complex in ATRP is the $[LCu^{I}]^{+}$.[75] In contrast, the deactivator complex requires the halide bound species in order to facilitate the deactivation of the propagating radical. Thus, a high halide concentration in solution is critical to favoring the deactivation of the propagating radical, and improving the control over dispersity.

Finally, acidic monomers such as acrylic acid and methacrylic acid have been a known problem for ATRP due to several reasons, including the protonation of the ligands at low pH leading to deactivation of the mediator complex,[76, 77] displacement of the halide anion from the deactivator complex,[77] and coordination of the carboxylate anion onto the mediator centers.[76] However, the problem of monomers bearing acidic functional groups was overcome in 2016 by Fantin et al[78] through the use of low pH in order to protonate the carboxylate and a chloro initiator to suppress background substitution cyclization of the chain end into the related lactone.

Conclusion and Outlook

ATRP was originally developed from atom transfer radical addition (ATRA). However, the last 25 years has seen massive improvements in ATRP catalyst activity due in large part to our improved understanding of structure-reactivity trends. Moreover, this has been accompanied by process developments such as AGET, ARGET, ICAR and SARA that allow for oxygen tolerance and ppm catalyst concentrations. These developments in carbon-halogen bond activation now offer new opportunities in small molecule synthesis. For example, in ATRA, the use of ATRP catalysts has led to reduced catalytic loading and lower temperatures in order to execute these transformations.[9] Another application of ATRP catalysts is in cross-coupling where the reactivity of a copper(III) intermediate in reductive elimination has recently been exploited in order to facilitate the room temperature coupling of alkyl halides to amides and heteroaromatic amines in high yields[79]. In this work, the catalyst activates the alkyl halide bonds in the normal manner and then Cu^{II} species coordinates both the nucleophile and radical, forming a short-lived Cu^{III} intermediate that rapidly undergoes reductive elimination (Scheme 6). Interestingly, this type of process has been observed as a minor side reaction in ATRP, where end-group analysis of PMMA revealed formation of a lactone.[78] Further exploration of this chemistry in couplings to other substrates, such as alkynes, is currently underway. As increasingly active catalysts are developed, the scope of these small molecule reactions, as well ATRP itself, will be further improved.

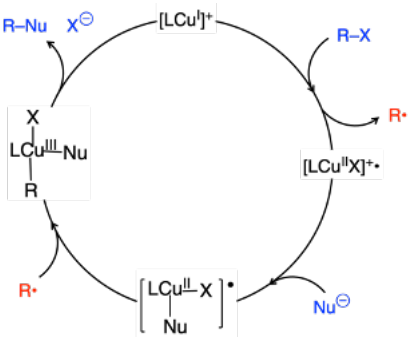

Scheme 6. ATRP-inspired cross-coupling cycle

Acknowledgments

MLC gratefully acknowledges an Australian Research Council Laureate Fellowship (FL170100041).

Supporting Information Available

An extensive compilation of R-H, R-Cl and R-Br bond dissociation Gibbs free energies, as taken from Refs 62-64 and used in the construction of Figures 3-4.

References

1 P. Nesvadba, Radical Polymerization in Industry, in *Encyclopedia of Radicals in Chemistry, Biology and Materials* (2012).
2 K. Matyjaszewski and J. Spanswick, *Mater Today* **8:**26-33 (2005).
3 W. A. Braunecker and K. Matyjaszewski, *Prog Polym Sci* **32:**93-146 (2007).
4 G. Moad and E. Rizzardo, *Macromolecules* **28:**8722-8728 (1995).
5 J. Chiefari, Y. K. Chong, F. Ercole, J. Krstina, J. Jeffery, T. P. T. Le, R. T. A. Mayadunne, G. F. Meijs, C. L. Moad, G. Moad, E. Rizzardo and S. H. Thang, *Macromolecules* **31:**5559-5562 (1998).
6 M. Kato, M. Kamigaito, M. Sawamoto and T. Higashimura, *Macromolecules* **28:**1721-1723 (1995).
7 J.-S. Wang and K. Matyjaszewski, *J Am Chem Soc* **117:**5614-5615 (1995).
8 F. di Lena and K. Matyjaszewski, *Prog Polym Sci* **35:**959-1021 (2010).
9 T. Pintauer and K. Matyjaszewski, *Chem Soc Rev* **37:**1087-1097 (2008).
10 C. Sambiagio, S. P. Marsden, A. J. Blacker and P. C. McGowan, *Chem Soc Rev* **43:**3525-3550 (2014).
11 J. M. Ahn, J. C. Peters and G. C. Fu, *J Am Chem Soc* **139:**18101-18106 (2017).
12 C. Y. Lin, M. L. Coote, A. Gennaro and K. Matyjaszewski, *J Am Chem Soc* **130:**12762-12774 (2008).
13 A. A. Isse, A. Gennaro, C. Y. Lin, J. L. Hodgson, M. L. Coote and T. Guliashvili, *J Am Chem Soc* **133:**6254-6264 (2011).
14 C. Fang, M. Fantin, X. C. Pan, K. de Fiebre, M. L. Coote, K. Matyjaszewski and P. Liu, *J Am Chem Soc* **141:**7486-7497 (2019).
15 V. Doan, B. B. Noble, A. K. K. Fung and M. L. Coote, *J Org Chem* **84:**15624-15632 (2019).
16 G. O. Jones, P. Liu, K. N. Houk and S. L. Buchwald, *J Am Chem Soc* **132:**6205-6213 (2010).
17 A. Bartoszewicz, C. D. Matier and G. C. Fu, *J Am Chem Soc* **141:**14864-14869 (2019).
18 J.-S. Wang and K. Matyjaszewski, *Macromolecules* **28:**7572-7573 (1995).
19 K. Matyjaszewski, S. Coca, S. G. Gaynor, M. Wei and B. E. Woodworth, *Macromolecules* **31:**5967-5969 (1998).
20 M. Li and K. Matyjaszewski, *Macromolecules* **36:**6028-6035 (2003).
21 J. Gromada and K. Matyjaszewski, *Macromolecules* **34:**7664-7671 (2001).
22 W. Jakubowski and K. Matyjaszewski, *Macromolecules* **38:**4139-4146 (2005).
23 K. Min, H. Gao and K. Matyjaszewski, *J Am Chem Soc* **127:**3825-3830 (2005).
24 W. Jakubowski, K. Min and K. Matyjaszewski, *Macromolecules* **39:**39-45 (2006).
25 K. Matyjaszewski, W. Jakubowski, K. Min, W. Tang, J. Huang, W. A. Braunecker and N. V. Tsarevsky, *Proc Nat Acad Sci* **103:**15309-15314 (2006).
26 M. Zhong and K. Matyjaszewski, *Macromolecules* **44:**2668-2677 (2011).
27 P. Krys, H. Schroeder, J. Buback, M. Buback and K. Matyjaszewski, *Macromolecules* **49:**7793-7803 (2016).
28 K. Matyjaszewski, S. Coca, S. G. Gaynor, M. Wei and B. E. Woodworth, *Macromolecules* **30:**7348-7350 (1997).
29 Y. Zhang, Y. Wang and K. Matyjaszewski, *Macromolecules* **44:**683-685 (2011).
30 V. Percec, T. Guliashvili, J. S. Ladislaw, A. Wistrand, A. Stjerndahl, M. J. Sienkowska, M. J. Monteiro and S. Sahoo, *J Am Chem Soc* **128:**14156-14165 (2006).
31 Y. Wang, M. Zhong, W. Zhu, C.-H. Peng, Y. Zhang, D. Konkolewicz, N. Bortolamei, A. A. Isse, A. Gennaro and K. Matyjaszewski, *Macromolecules* **46:**3793-3802 (2013).
32 C.-H. Peng, M. Zhong, Y. Wang, Y. Kwak, Y. Zhang, W. Zhu, M. Tonge, J. Buback, S. Park, P. Krys, D. Konkolewicz, A. Gennaro and K. Matyjaszewski, *Macromolecules* **46:**3803-3815 (2013).
33 D. Konkolewicz, Y. Wang, M. Zhong, P. Krys, A. A. Isse, A. Gennaro and K. Matyjaszewski, *Macromolecules* **46:**8749-8772 (2013).
34 G. Lligadas, S. Grama and V. Percec, *Biomacromolecules* **18:**2981-3008 (2017).
35 D. Konkolewicz, Y. Wang, P. Krys, M. Zhong, A. A. Isse, A. Gennaro and K. Matyjaszewski, *Polym Chem* **5:**4396-4417 (2014).

36 P. Chmielarz, M. Fantin, S. Park, A. A. Isse, A. Gennaro, A. J. D. Magenau, A. Sobkowiak and K. Matyjaszewski, *Prog Polym Sci* **69:**47-78 (2017).
37 M. A. Tasdelen, M. Uygun and Y. Yagci, *Macromol Rapid Commun* **32:**58-62 (2011).
38 H. Mohapatra, M. Kleiman and A. P. Esser-Kahn, *Nat Chem* **9:**135-139 (2017).
39 C. Boyer, N. A. Corrigan, K. Jung, D. Nguyen, T.-K. Nguyen, N. N. M. Adnan, S. Oliver, S. Shanmugam and J. Yeow, *Chem Rev* **116:**1803-1949 (2016).
40 X. Pan, M. A. Tasdelen, J. Laun, T. Junkers, Y. Yagci and K. Matyjaszewski, *Prog Polym Sci* **62:**73-125 (2016).
41 G. Kickelbick, T. Pintauer and K. Matyjaszewski, *New J Chem* **26:**462-468 (2002).
42 G. Mazzotti, T. Benelli, M. Lanzi, L. Mazzocchetti and L. Giorgini, *Eur Polym J* **77:**75-87 (2016).
43 H. Tang, M. Radosz and Y. Shen, *AIChE Journal* **55:**737-746 (2009).
44 P. Liu and Z. Su, *Polym Int* **54:**1508-1511 (2005).
45 G. L. Cheng, C. P. Hu and S. K. Ying, *Macromol Rapid Commun* **20:**303-307 (1999).
46 Q. Yang, J. Lalevée and J. Poly, *Macromolecules* **49:**7653-7666 (2016).
47 Q. Yang, F. Dumur, F. Morlet-Savary, J. Poly and J. Lalevée, *Macromolecules* **48:**1972-1980 (2015).
48 J. Xia and K. Matyjaszewski, *Macromolecules* **30:**7697-7700 (1997).
49 J. Xia and K. Matyjaszewski, *Macromolecules* **32:**2434-2437 (1999).
50 J. Xia, S. G. Gaynor and K. Matyjaszewski, *Macromolecules* **31:**5958-5959 (1998).
51 T. G. Ribelli, M. Fantin, J.-C. Daran, K. F. Augustine, R. Poli and K. Matyjaszewski, *J Am Chem Soc* **140:**1525-1534 (2018).
52 A. E. Enciso, F. Lorandi, A. Mehmood, M. Fantin, G. Szczepaniak, B. G. Janesko and K. Matyjaszewski, *Angew Chem Int Ed* https://doi.org/10.1002/ange.202004724 (2020).
53 J. Qiu, K. Matyjaszewski, L. Thouin and C. Amatore, *Macromol Chem Phys* **201:**1625-1631 (2000).
54 W. A. Braunecker, W. C. Brown, B. C. Morelli, W. Tang, R. Poli and K. Matyjaszewski, *Macromolecules* **40:**8576-8585 (2007).
55 M. Hossain, M. Rahman, B. Mohon Chaki, M. Rahman, M. Miah and H. Ahmad, *J Polym Mater* **24:**101 (2007).
56 S. C. Hong, H. J. Kim, Y. R. Lee, S. Noh and W. S. Lyoo, *J Ind Eng Chem* **12:**60-68 (2006).
57 S. C. Hong, K. E. Shin, S. K. Noh and W. S. Lyoo, *Macromol Res* **13:**391-396 (2005).
58 W. Tang, Y. Kwak, W. Braunecker, N. V. Tsarevsky, M. L. Coote and K. Matyjaszewski, *J Am Chem Soc* **130:**10702-10713 (2008).
59 K. Matyjaszewski, B. Göbelt, H.-j. Paik and C. P. Horwitz, *Macromolecules* **34:**430-440 (2001).
60 J. Xia, X. Zhang and K. Matyjaszewski, The Effect of Ligands on Copper-Mediated Atom Transfer Radical Polymerization, in *Transition Metal Catalysis in Macromolecular Design*. American Chemical Society, pp. 207-223 (2000).
61 W. Tang and K. Matyjaszewski, *Macromolecules* **39:**4953-4959 (2006).
62 M. L. Coote, C. Y. Lin and A. A. Zavitsas, *Phys Chem Chem Phys* **16:**8686-8696 (2014).
63 M. L. Coote, C. Y. Lin, A. L. J. Beckwith and A. A. Zavitsas, *Phys Chem Chem Phys* **12:**9597-9610 (2010).
64 C. Y. Lin, S. R. A. Marque, K. Matyjaszewski and M. L. Coote, *Macromolecules* **44:**7568-7583 (2011).
65 C. Hansch, A. Leo and R. W. Taft, *Chem Rev* **91:**165-195 (1991).
66 K. S. Root, C. L. Hill, L. M. Lawrence and G. M. Whitesides, *J Am Chem Soc* **111:**5405-5412 (1989).
67 M. Fantin, F. Lorandi, T. G. Ribelli, G. Szczepaniak, A. E. Enciso, C. Fliedel, L. Thevenin, A. A. Isse, R. Poli and K. Matyjaszewski, *Macromolecules* **52:**4079-4090 (2019).
68 A. J. D. Magenau, N. C. Strandwitz, A. Gennaro and K. Matyjaszewski, *Science* **332:**81-84 (2011).
69 Z. Wang, X. Pan, L. Li, M. Fantin, J. Yan, Z. Wang, Z. Wang, H. Xia and K. Matyjaszewski, *Macromolecules* **50:**7940-7948 (2017).
70 J. T. Hupp and M. J. Weaver, *Inorg Chem* **23:**3639-3644 (1984).
71 H. Svith, H. Jensen, J. Almstedt, P. Andersson, T. Lundbäck, K. Daasbjerg and M. Jonsson, *J Phys Chem A* **108:**4805-4811 (2004).

72 W. A. Braunecker, N. V. Tsarevsky, A. Gennaro and K. Matyjaszewski, *Macromolecules* **42:**6348-6360 (2009).
73 G. Coullerez, E. Malmström and M. Jonsson, *J Phys Chem A* **110:**10355-10360 (2006).
74 M. Horn and K. Matyjaszewski, *Macromolecules* **46:**3350-3357 (2013).
75 N. Bortolamei, A. A. Isse, V. B. Di Marco, A. Gennaro and K. Matyjaszewski, *Macromolecules* **43:**9257-9267 (2010).
76 H. Mori and A. H. E. Müller, *Prog Polym Sci* **28:**1403-1439 (2003).
77 M. Fantin, A. A. Isse, A. Gennaro and K. Matyjaszewski, *Macromolecules* **48:**6862-6875 (2015).
78 M. Fantin, A. A. Isse, A. Venzo, A. Gennaro and K. Matyjaszewski, *J Am Chem Soc* **138:**7216-7219 (2016).
79 A. K. K. Fung, L.-J. Yu and M. L. Coote, *submitted* (2020).